
Joint Communication and Sensing with Bipartite Entanglement over Bosonic Channels

Tuna Erdoğan, Shi-Yuan Wang, Shang-Jen Su, Matthieu Bloch

Abstract

We consider a joint communication and sensing problem in an optical link in which a low-power transmitter attempts to communicate with a receiver while simultaneously identifying the range of a defect creating a backscattered signal. We model the system as a lossy thermal noise bosonic channel in which the location of the target, modeled as a beamsplitter, affects the timing of the backscattered signal. Motivated by the envisioned deployment of entanglement sharing quantum networks, we allow the transmitter to exploit entanglement to assist its sensing and communication. Since entanglement is known to enhance sensing, as known from quantum illumination, and increase communication rates, as known from the characterization of the entanglement-assisted capacity, the transmitter is faced with a trade-off and must judiciously allocate its entanglement resources. Our main result is a characterization of the trade-offs incurred in the form of an achievable rate/error-exponent region which can beat time-sharing in certain cases. The proof of our result relies on technical results of independent interests, by which we carefully show how to extend the known asymptotic characterization of multi-hypothesis testing Chernoff exponent in finite-dimensional spaces to infinite-dimensional spaces and provide a characterization of phase shift keying modulated displaced thermal states in Fock basis.

1 Introduction

Although the vision of the Quantum Internet as an ubiquitous network connecting distant quantum computers and sensors is still decades away, there have been recent significant advances towards a first-generation Quantum Internet in the form of an entanglement-sharing network [1]. In particular, we now have a deeper understanding of how to efficiently distribute entanglement over long distances by appropriately processing shared entanglement between neighboring nodes [2]. A key aspect of these recent works, however, is to treat entanglement as a resource to be consumed without considering the nature of the tasks consuming entanglement. As long as entanglement-sharing remains costly, efficient use of entanglement is likely to require a careful allocation of entanglement resources across tasks.

Our objective is to develop preliminary insights into the resulting performance trade-offs that would result from this operation by formulating an exemplar combining two entanglement-assisted tasks: sensing and communication. This exemplar is motivated by recent experimental results reporting joint communication and sensing in optical links [3], as well as the usefulness of entanglement to improve detection in quantum illumination [4] and increase communication rates over bosonic channels [5]. This model extends our prior work on joint communication and sensing that only considered finite-dimensional Hilbert spaces and did not include entanglement assistance [6], and extends recent independently obtained results on joint communication and sensing over lossy bosonic channels without entanglement [7]. The problem of joint communication and sensing has been investigated in classical information theory for Discrete Memoryless Channels (DMCs) under various models: capacity/distortion/cost trade-offs for independent and identically distributed (i.i.d.) channel states [8], rate/error-exponent trade-offs for binary channel states [9] and rate/error-exponent tradeoffs under monostatic and bistatic detection models [10, 11].

Here, we consider a lossy thermal noise bosonic channel in which a transmitter simultaneously wishes to communicate with a receiver and range the location of the beamsplitter [12]. The operation of the transmitter is assisted by an entangled state from a Two-Mode Squeezed Vacuum (TMSV) source [13] consisting of a signal and idler pair. The transmitter encodes information on the signal but is faced with a dilemma with respect to the idler: it can transmit the idler to the receiver, i.e., through an entanglement sharing network, to enable entanglement-assisted communication or it can keep the idler, i.e. in a local quantum memory, to enable quantum illumination. We provide insights into the incurred performance trade-offs in the form of an achievable communication rate/sensing exponent. As a necessary step towards developing this result, we carefully extend the characterization of the multiple hypothesis testing Chernoff exponent [14] to infinite-dimensional spaces. Our result extends a recently obtained similar extension for pure loss bosonic channels [15]. The crux of our approach is to project on a finite-dimensional space and invoke a continuity property of the Chernoff information.

The remainder of the paper is organized as follows. We formally introduce the notation and model of interest in Section 2. We extend [14, Theorem 1] to infinite-dimensional spaces in Section 3, which might be of independent interest. We present our main results regarding the joint communication and sensing trade-off in Section 4 and defer proofs to Section 5 to streamline presentation. This article could be found with the following URL <https://bloch.ece.gatech.edu/JointBosonicCommSensing.pdf>.

2 Notation and Joint Communication and Sensing Model

2.1 Notation

Let \mathbb{R}_+ and \mathbb{N}_* denote the sets of non-negative real numbers and positive integers, respectively. For any set \mathcal{X} and $n \in \mathbb{N}_*$ a sequence of n elements is denoted by $x^n = (x_1, \dots, x_n) \in \mathcal{X}^n$. For any n and k such that $n \leq k$, $x^{n:k} \triangleq (x^n, \dots, x^k)$. Moreover, for any $a, b \in \mathbb{R}$ such that $\lfloor a \rfloor \leq \lceil b \rceil$, we define $\llbracket a, b \rrbracket \triangleq \{\lfloor a \rfloor, \lfloor a \rfloor + 1, \dots, \lceil b \rceil - 1, \lceil b \rceil\}$. Throughout the paper, $\log(\cdot)$ is with respect to (w.r.t.) base e , and therefore all the information quantities should be understood in *nats*.

Let $\mathcal{D}(\mathcal{H})$ denote the set of density operators acting on a *separable* Hilbert space \mathcal{H} . Let $\mathbb{1}_{\mathcal{H}}$ denote the identity operator acting on \mathcal{H} . The von Neumann entropy of $\hat{\rho} \in \mathcal{D}(\mathcal{H})$ is $S(\hat{\rho}) \triangleq -\text{tr}(\hat{\rho} \log \hat{\rho})$. The Holevo information of a Classical-Quantum (c-q) ensemble $\{p_X(x), \hat{\rho}^x\}$ is $\chi(\{p_X(x), \hat{\rho}^x\}) \triangleq S(\sum_x p_X(x) \hat{\rho}^x) - \sum_x p_X(x) S(\hat{\rho}^x)$. In a bosonic system, self-adjoint canonical operators of position \hat{q} and momentum \hat{p} satisfy $[\hat{q}, \hat{p}] = i\hbar$, where \hbar is the reduced Planck constant and we let $\hbar = 1$ in appropriate units. Through the canonical operators the creation and annihilation operators are defined as $\hat{a}^\dagger \triangleq \frac{\hat{q} + i\hat{p}}{\sqrt{2}}$ and $\hat{a} \triangleq \frac{\hat{q} - i\hat{p}}{\sqrt{2}}$, respectively. For $\alpha \in \mathbb{C}$ the one mode displacement operator is $\hat{D}(\alpha) \triangleq \exp(\alpha \hat{a}^\dagger - \alpha^* \hat{a})$. The photon number operator is $\hat{N} \triangleq \hat{a}^\dagger \hat{a}$.

2.2 Joint Communication and Sensing Model with Bipartite Entanglement Resource

We consider the problem of joint communication and sensing over multiple uses of a single-mode lossy thermal noise bosonic channel $\mathcal{L}_{A \rightarrow BD}^{(\eta, N_{\text{th}}/\eta)}$, where η is the transmissivity and N_{th}/η is the mean photon number of the thermal noise. A transmitter (Alice) attempts to reliably transmit a uniformly distributed message W to a receiver (Bob) while performing hypothesis testing on the range the of the beamsplitter through the returned signal of the channel while being subject to mean photon number constraint N . The joint communication and sensing model over a lossy thermal-noise bosonic channel is given in Figure 1.

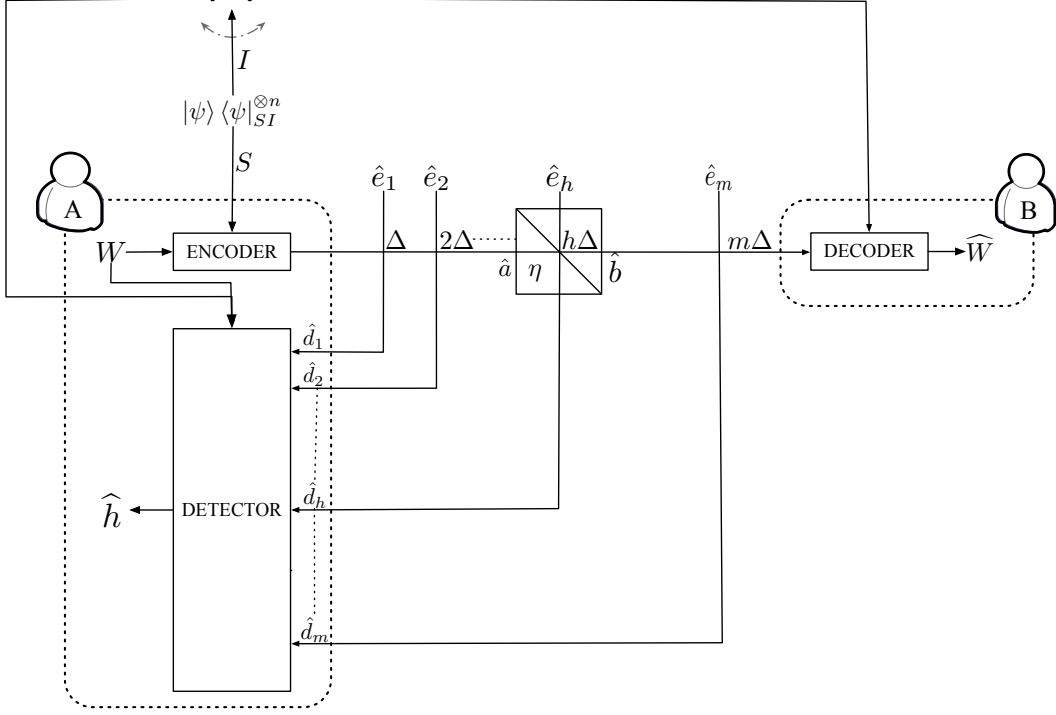


Figure 1: Joint communication and sensing model with entanglement resource over a lossy thermal-noise bosonic channel.

Alice is simultaneously trying to reliably transmit the uniform message $W \in \llbracket 1, M \rrbracket$ and determine the position of the beamsplitter in her line of sight. Motivated by the ranging formulation in [12], the ranging problem is formulated as multiary hypothesis testing problem. The known distance between Alice and Bob is split into $m + 1$ slices, $m \geq 2$, each of length Δ . In hypothesis $h \in \llbracket 1, m \rrbracket$, the beamsplitter is at position $h\Delta$. Alice's channel observations are modes $\{\hat{d}_i\}_{i=1}^h$ each arriving in between $t \in [2i\frac{\Delta}{c}, 2(i+1)\frac{\Delta}{c})$ for $i \in \llbracket 1, m \rrbracket$.

The relationship of the annihilation operators of the bosonic modes in hypothesis h are

$$\hat{b} = \sqrt{\eta}\hat{a} + \sqrt{1-\eta}\hat{e}_h, \quad (1)$$

$$\hat{d}_h = -\sqrt{1-\eta}\hat{a} + \sqrt{\eta}\hat{e}_h, \quad (2)$$

$$\hat{d}_i = \hat{e} \quad \forall i \neq h. \quad (3)$$

As in [12] we adopt the assumption of No Passive Signature (NPS), in which \hat{e}_h is a thermal state with mean photon number $\frac{N_{\text{th}}}{\eta}$ and \hat{e} is a thermal state with mean photon number N_{th} under hypothesis h . The thermal state with mean photon number N_{th} is given by

$$\hat{\rho}_{\text{th}}(N_{\text{th}}) \triangleq \sum_{n=0}^{\infty} \frac{N_{\text{th}}^n}{(N_{\text{th}} + 1)^{n+1}} |n\rangle \langle n| \quad (4)$$

$$= \frac{1}{\pi N_{\text{th}}} \int \exp\left(-\frac{|\beta|^2}{N_{\text{th}}}\right) |\beta\rangle \langle \beta| d^2\beta. \quad (5)$$

Alice has access to a two-mode squeezed vacuum (TMSV) entangled state $\hat{\rho}_{SI}^{\otimes n}$, where $\hat{\rho}_{SI} = |\psi\rangle\langle\psi|_{SI}$

$$|\psi\rangle_{SI} = \sum_{n=0}^{\infty} \sqrt{\frac{N_S^n}{(N_S+1)^{n+1}}} |n\rangle_S |n\rangle_I, \quad (6)$$

which she can choose to share with Bob to assist the transmission of her uniform message $W \in \llbracket 1, M \rrbracket$ or to enhance her hypothesis testing. We consider schemes that do not "split" the entanglement, i.e., during a fraction λ of the blocklength n Alice shares the idler with Bob to assist the transmission of her encoded message and during the remaining fraction $(1 - \lambda)$ she uses the idler to enhance ranging performance.

Alice's encoder consists of two parts:

1. For the first λn modes she encodes her classical message via Phase Shift Keying (PSK) by applying a single mode phase shift unitary $\hat{U}_\theta \triangleq \exp(i\theta \hat{a}^\dagger \hat{a})$ to each mode,
2. For the remaining $(1 - \lambda)n$ modes she encodes the classical message via displaced PSK by applying a single mode displacement unitary $\hat{D}(|\alpha| e^{i\theta})$ to each signal mode,

where $\theta \in [0, 2\pi]$ is uniformly distributed in both cases. Therefore, Alice's encoder is described by the encoder channels $\{\mathcal{E}_{S^n \rightarrow A^n}^{(w, \lambda)} \otimes \mathbb{1}_{I^n}\}$ mapping the message $w \in \llbracket 1, M \rrbracket$ to an n mode state $\hat{\rho}_{A^n I^n}^{(w, \lambda)}$ entangled with the idler I . Explicitly,

$$\mathcal{E}_{S^n \rightarrow A^n}^{(w, \lambda)} = \left(\bigotimes_{j=1}^{\lambda n} \hat{U}_{\theta_j(w)} \right) \otimes \left(\bigotimes_{k=\lambda n+1}^n \hat{D}(|\alpha| e^{i\theta_k(w)}) \right), \quad (7)$$

in which $\theta_{\lambda n+1}(w) = 0$ as a phase reference for the displaced PSK scheme. The modulation by displacement introduces a new variable $N_m \triangleq |\alpha|^2$, where "m" stands for modulation. N_m identifies the power injected into the channel because of the displacement and the total mean photon number constraint of the channel becomes $N_S + N_m \leq N$.

Upon observing the channel output $\hat{\rho}_{B^n I^{1:\lambda n}}^{(w, \lambda)} \triangleq \text{tr}_{D^n, I^{\lambda n+1:n}} \left(\left(\left(\mathcal{L}_{A \rightarrow BD}^{(\eta, N_B)} \right)^{\otimes n} \otimes \mathbb{1}_{I^n} \right) \hat{\rho}_{A^n I^n}^{(w, \lambda)} \right)$,

Bob applies Positive Operator-Valued Measure (POVM) $\{\Pi_{B^n, I^{1:\lambda n}}^{(w, \lambda)}\}_{w=1}^M$ on the received signal to obtain an estimate \widehat{W} of the message W . Similarly, upon receiving the returned state under hypothesis h

$$\begin{aligned} \hat{\rho}_{\{D_j^n\}_{j=1}^m I^{\lambda n+1:n}}^{(h, w, \lambda)} &\triangleq (\hat{\rho}_{\text{th}}(N_{\text{th}})^{\otimes n})^{\otimes h-1} \otimes \left(\text{tr}_{B^n, I^{1:\lambda n}} \left(\left(\left(\mathcal{L}_{A \rightarrow BD}^{(\eta, N_B)} \right)^{\otimes n} \otimes \mathbb{1}_{I^n} \right) \hat{\rho}_{A^n I^n}^w \right) \right) \\ &\otimes (\hat{\rho}_{\text{th}}(N_{\text{th}})^{\otimes n})^{\otimes m-h}, \end{aligned} \quad (8)$$

Alice obtains estimate an \hat{h} of the true hypothesis by applying POVM $\left\{ \Lambda_{\{D_j^n\}_{j=1}^m I^{\lambda n+1:n}}^{(h, w, \lambda)} \right\}$. We define the communication rate

$$R \triangleq \frac{\log M}{n}, \quad (9)$$

and measure the reliability using the maximum probability error

$$P_{e,c}^n \triangleq \max_{w \in \llbracket 1, M \rrbracket} \text{tr} \left(\left(\mathbb{1}_{B^n, I^{1:\lambda n}} - \Pi_{B^n, I^{1:\lambda n}}^{(w, \lambda)} \right) \hat{\rho}_{B^n I^{1:\lambda n}}^{(w, \lambda)} \right). \quad (10)$$

We measure the sensing performance using the maximum probability of error for hypothesis testing

$$P_{e,d}^n \triangleq \max_{h \in \llbracket 1, m \rrbracket} \max_{w \in \llbracket 1, M \rrbracket} \text{tr} \left(\left(\mathbb{1}_{\{D_j^n\}_{j=1}^m I^{\{\lambda_{n+1:n}\}} - \Lambda_{\{D_j^n\}_{j=1}^m I^{\{\lambda_{n+1:n}\}}^h \right) \hat{\rho}_{\{D_j^n\}_{j=1}^m I^{\{\lambda_{n+1:n}\}}}^{(h,w,\lambda)} \right) \right) \quad (11)$$

and define the sensing error exponent as

$$E \triangleq \lim_{n \rightarrow \infty} -\frac{\log P_{e,d}^n}{n}. \quad (12)$$

We restrict our attention to the low signal-to-noise ratio regime in which $N_S \ll 1 \ll N_B$ and $1 - \eta \ll 1$ since this regime is where the advantage of entanglement is most apparent.

3 Preliminaries: Multiple Hypothesis Testing in Infinite-dimension

The characterization of the asymptotic performance of binary hypothesis tests for quantum states and channels is now well understood [16]. The generalization of these results to multiple hypotheses presents additional challenges, and while the expression for the Chernoff exponent in [14, Theorem 1] parallels its classical counterpart [17, Theorem 1], the proof is significantly more involved and explicitly relies on the finite-dimensional nature of the underlying Hilbert space. While it might be reasonable to believe that [14, Theorem 1] holds for infinite-dimensional Hilbert spaces, there is no formal proof of this result to our knowledge. We provide such extension in the next theorem.

Theorem 3.1. *Let $\{\hat{\rho}_i\}_{i=1}^m$ be a finite set of quantum states on a Hilbert space \mathcal{H} . The asymptotic error exponent for testing $\{\hat{\rho}_i^{\otimes n}\}_{i=1}^m$, for an arbitrary non-degenerate prior $\{\pi_i\}_{i=1}^m$ is given by*

$$\lim_{n \rightarrow \infty} -\frac{1}{n} \log P_e^n \left(\{\pi_i \hat{\rho}_i^{\otimes n}\}_{i=1}^m \right) = \min_{(i,j): i \neq j} \max_{s \in [0,1]} -\log \text{tr} \left(\hat{\rho}_i^s \hat{\rho}_j^{1-s} \right), \quad (13)$$

$$\triangleq \min_{(i,j): i \neq j} \max_{s \in [0,1]} -\log Q_s \left(\hat{\rho}_i \| \hat{\rho}_j \right). \quad (14)$$

Remark 3.2. *We can use the similar techniques for the achievability proof of f -divergences, specifically Rényi divergences.*

We also extend the controlled sensing result for multiple quantum hypothesis testing from [6, Theorem 4.1], when a control input $x \in \mathcal{X}$, $|\mathcal{X}| < \infty$ and a given hypothesis i result in the generation of a state with density matrix $\hat{\rho}_i^x$.

Theorem 3.3. *Let $\{\{\hat{\rho}_i^x\}_{x \in \mathcal{X}}\}_{i=1}^m$ be a finite set of quantum states on a Hilbert space \mathcal{H} with control inputs $x \in \mathcal{X}$, $|\mathcal{X}| < \infty$. The asymptotic error exponent for testing $\{\hat{\rho}_i^x\}_{i=1}^m$, for an arbitrary non-degenerate prior $\{\pi_i\}_{i=1}^m$ and a control sequence $\{x_n\}_{n \in \mathbb{N}_*}$ with fixed empirical distribution p_X is given by*

$$\lim_{n \rightarrow \infty} -\frac{1}{n} \log P_e^n \left(\{\pi_i \hat{\rho}_i^{x_n}\}_{i=1}^m \right) = \min_{(i,j): i \neq j} \max_{s \in [0,1]} - \sum_{x \in \mathcal{X}} p_X(x) \log \text{tr} \left((\hat{\rho}_i^x)^s (\hat{\rho}_j^x)^{1-s} \right), \quad (15)$$

$$= \min_{(i,j): i \neq j} \max_{s \in [0,1]} - \sum_{x \in \mathcal{X}} p_X(x) \log Q_s \left(\hat{\rho}_i^x \| \hat{\rho}_j^x \right). \quad (16)$$

Remark 3.4. *The restriction to finite control alphabet in Theorem 3.3 is the reason we use a displaced PSK defined in Section 2.2 instead of the standard Gaussian modulated coherent state encoding.*

Remark 3.5. *The proof of Theorem 3.3 uses the same techniques that are used in the proof of Theorem 3.1, so we only provide proof of the former.*

3.1 Achievability Proof of Theorem 3.1

The idea is to apply an N -dimensional projection $\{\Pi_N\}_{N \in \mathbb{N}_*}$ to the received state and then perform the m -ary hypothesis testing on the projected states. Applying [14, Theorem 1] to truncated states $\{\pi_i \Pi_N^{\otimes n} \hat{\rho}_i^{\otimes n} \Pi_N^{\otimes n}\}_{i=1}^m$

$$\lim_{n \rightarrow \infty} -\frac{1}{n} \log P_e^n \left(\{\pi_i \Pi_N^{\otimes n} \hat{\rho}_i^{\otimes n} \Pi_N^{\otimes n}\}_{i=1}^m \right) = \min_{(i,j): i \neq j} \max_{s \in [0,1]} -\log Q_s (\Pi_N \hat{\rho}_i \Pi_N \| \Pi_N \hat{\rho}_j \Pi_N) \quad (17)$$

Now we need to show the continuity of the right hand side of (17) as $N \rightarrow \infty$. [18, Lemma 5.2] shows that for states ρ and σ , $Q_s(\rho \| \sigma)$ is an f -divergence.

Lemma 3.6 ([18, Lemma 5.2]). *Define the convex functions f_s on $[0, \infty)$ by*

$$f_s(t) = \begin{cases} t^s & \text{if } s \geq 1, \\ -t^s & \text{if } s \in (0, 1). \end{cases} \quad (18)$$

Then, for any two states ρ, σ , we have

$$Q_s(\rho \| \sigma) = \begin{cases} S_{f_s}(\rho \| \sigma) & \text{if } s \geq 1, \\ -S_{f_s}(\rho \| \sigma) & \text{if } s \in (0, 1). \end{cases} \quad (19)$$

Furthermore, [18, Theorem 4.5] shows that for any two states ρ, σ the f -divergences are convergent under projections converging in strong operator topology to identity,

Theorem 3.7 ([18, Theorem 4.5]). *Let $\{e_\alpha\}_\alpha$ be an increasing net of projections in M such that $e_\alpha \rightarrow 1$. Then for every $\rho, \sigma \in M_*^+$,*

$$\lim_{\alpha} S_f(e_\alpha \rho e_\alpha \| e_\alpha \sigma e_\alpha) = S_f(\rho \| \sigma). \quad (20)$$

Hence, from [18, Theorem 4.5] and since $\{\Pi_N\}_{N \in \mathbb{N}_*}$ converges to the identity in the strong operator topology [18]

$$\lim_{N \rightarrow \infty} Q_s(\Pi_N \hat{\rho}_i \Pi_N \| \Pi_N \hat{\rho}_j \Pi_N) = Q_s(\hat{\rho}_i \| \hat{\rho}_j). \quad (21)$$

Property (2) of [18, Proposition 5.3] also shows that $\log Q_s(\hat{\rho}_i \| \hat{\rho}_j)$ is convex in s for $s \in [0, \infty)$, thus $\log Q_s(\hat{\rho}_i \| \hat{\rho}_j)$ is continuous in s for $s \in (0, 1]$. By continuity of $\log(\cdot)$,

$$\lim_{N \rightarrow \infty} \log Q_s(\Pi_N \hat{\rho}_i \Pi_N \| \Pi_N \hat{\rho}_j \Pi_N) = \log Q_s(\hat{\rho}_i \| \hat{\rho}_j). \quad (22)$$

To prove the continuity of $\min_{s \in [0,1]} \log Q_s(\hat{\rho}_i \| \hat{\rho}_j)$ we use the next theorem,

Theorem 3.8 ([19, Theorem 10.8]). *Let \mathcal{C} be a relatively open convex set, and let $\{f_n\}_{n \in \mathbb{N}^*}$ be a sequence of finite convex functions on \mathcal{C} . Suppose that the sequence converges pointwise on a dense subset of \mathcal{C} , i.e. that there exists a subset \mathcal{C}' of \mathcal{C} such that $\text{cl} \mathcal{C}' \supset \mathcal{C}$ and, for each $x \in \mathcal{C}'$, the limit of $\{f_n\}_{n \in \mathbb{N}^*}$ exists and is finite. The limit then exists for every $x \in \mathcal{C}$, and the function f , where*

$$f(x) = \lim_{n \rightarrow \infty} f_n(x) \quad (23)$$

is finite and convex on \mathcal{C} . Moreover the sequence $\{f_n\}_{n \in \mathbb{N}^}$ converges to f uniformly on each closed bounded subset of \mathcal{C} .*

From the above theorem for every density operator ρ, σ , the convergence in (22) is uniform on every compact subset of $(0, 1)$. For every $\delta > 0$ and for every $s \in [\delta, 1 - \delta]$ the convergence in (22) is uniform. Hence for every $\epsilon > 0$ there exists N_ϵ such that, for all $N > N_\epsilon$ and for all density operators $\rho \neq \sigma$,

$$\left| \min_{s \in [\delta, 1-\delta]} -\log Q_s(\Pi_N \rho \Pi_N \| \Pi_N \sigma \Pi_N) - \min_{s \in [\delta, 1-\delta]} -\log Q_s(\rho \| \sigma) \right| \leq \epsilon. \quad (24)$$

Since this is true for every ρ, σ and $\epsilon > 0$, and $\{0, 1\} \in \operatorname{argmin}_{s \in [0, 1]} \log Q_s(\Pi_N \rho \Pi_N \| \Pi_N \sigma \Pi_N)$ if and only if $\rho = \sigma$, for every $\epsilon > 0$, for all $N > N_\epsilon$ and for all density operators $\rho \neq \sigma$

$$\left| \min_{s \in (0, 1)} -\log Q_s(\Pi_N \rho \Pi_N \| \Pi_N \sigma \Pi_N) - \min_{s \in (0, 1)} -\log Q_s(\rho \| \sigma) \right| \leq \epsilon. \quad (25)$$

In the case $\rho = \sigma$, for all $N \in \mathbb{N}^*$

$$\log Q_s(\Pi_N \rho \Pi_N \| \Pi_N \sigma \Pi_N) = \log Q_s(\rho \| \sigma) = 0, \quad (26)$$

therefore

$$\left| \min_{s \in [0, 1]} \log Q_s(\Pi_N \rho \Pi_N \| \Pi_N \sigma \Pi_N) - \min_{s \in [0, 1]} \log Q_s(\rho \| \sigma) \right| \leq \epsilon. \quad (27)$$

Finally, let \mathcal{P} denote the set of unordered pairs of indices in $\llbracket 1, m \rrbracket$, i.e., $\mathcal{P} \triangleq \{(k, \ell) | k, \ell \in \llbracket 1, m \rrbracket, \ell < k\}$ and let the bijective mapping $\alpha : \mathcal{P} \rightarrow \llbracket 1, \frac{m(m-1)}{2} \rrbracket$ be the indexing of the unordered pairs. Now define $\frac{m(m-1)}{2}$ functions $f_{\alpha(i, j)}(\{\hat{\rho}_k\}_{k=1}^m) \triangleq \min_{s \in [0, 1]} -\log Q_s(\hat{\rho}_i \| \hat{\rho}_j)$. The minimum of two continuous functions is continuous, as seen from the equivalent representation of the pairwise min function,

$$\min(f, g) = \frac{f + g - |f - g|}{2}. \quad (28)$$

The minimization of the $\frac{m(m-1)}{2}$ functions $\{f_i\}_{i \in \llbracket 1, \frac{m(m-1)}{2} \rrbracket}$ can be defined inductively by defining

$$\tilde{f}_2 \triangleq \min(f_1, f_2), \quad (29)$$

$$\tilde{f}_i \triangleq \min\left(f_i, \tilde{f}_{i-1}\right), \quad \forall i \in \llbracket 3, \frac{m(m-1)}{2} \rrbracket. \quad (30)$$

\tilde{f}_i is then continuous for every $i \in \llbracket 1, \frac{m(m-1)}{2} \rrbracket$. In particular, $\tilde{f}_{\frac{m(m-1)}{2}} = \min_{i \neq j} f_{\alpha(i, j)}$ is continuous with respect to states $\{\hat{\rho}_k\}_{k=1}^m$. There for any m states $\{\hat{\rho}_i\}_{i \in \llbracket 1, m \rrbracket}$, for every $\epsilon > 0$, there exists N_ϵ such that

$$\left| \min_{i \neq j} \min_{s \in [0, 1]} -\log Q_s(\Pi_N \hat{\rho}_i \Pi_N \| \Pi_N \hat{\rho}_j \Pi_N) - \min_{i \neq j} \min_{s \in [0, 1]} -\log Q_s(\hat{\rho}_i \| \hat{\rho}_j) \right| \leq \epsilon. \quad (31)$$

3.2 Converse Proof of Theorem 3.1

Reduction to a Binary Hypothesis Testing: We use the proof technique in [20, Theorem 1] to show that, for any sequence of POVM discriminating the m -ary hypotheses, the probability of error for detection can be lower bounded by that of a binary hypothesis test between any pair of hypotheses.

Consider the POVM $\{\Pi_i\}_{i \in \llbracket 1, m \rrbracket}$ and a fixed pair of indices $i \neq j \in \llbracket 1, m \rrbracket$. Let $A, B \in \mathcal{P}(\mathcal{H}^{\otimes n})$ be such that $A + B = \mathbb{1} - \Pi_i - \Pi_j$. We construct a new POVM for binary hypothesis testing for $\hat{\rho}_i^{\otimes n}$ vs $\hat{\rho}_j^{\otimes n}$ by defining $\tilde{\Pi}_i \triangleq \Pi_i + A$ and $\tilde{\Pi}_j \triangleq \Pi_j + B$.

Next, we show that the error of the new hypothesis test is a lower bound on the error probability of the original test. Since $\tilde{\Pi}_i \succeq \Pi_i$ by monotonicity we have $\text{tr}(\hat{\rho}_i^{\otimes n}(\mathbb{1} - \tilde{\Pi}_i)) \leq \text{tr}(\hat{\rho}_i^{\otimes n}(\mathbb{1} - \Pi_i))$. Then,

$$P_e^n \left(\left\{ \{\pi_k \hat{\rho}_k^{\otimes n}\}_{k \in \llbracket 1, m \rrbracket}; \{\Pi_k\}_{k \in \llbracket 1, m \rrbracket} \right\} \right) \geq \pi_i \text{tr}(\hat{\rho}_i^{\otimes n}(\mathbb{1} - \Pi_i)) + \pi_j \text{tr}(\hat{\rho}_j^{\otimes n}(\mathbb{1} - \Pi_j)) \quad (32)$$

$$\geq \pi_i \text{tr}(\hat{\rho}_i^{\otimes n}(\mathbb{1} - \tilde{\Pi}_i)) + \pi_j \text{tr}(\hat{\rho}_j^{\otimes n}(\mathbb{1} - \tilde{\Pi}_j)) \quad (33)$$

$$\geq \min(\pi_i, \pi_j) \left(\text{tr}(\hat{\rho}_i^{\otimes n}(\mathbb{1} - \tilde{\Pi}_i)) + \text{tr}(\hat{\rho}_j^{\otimes n}(\mathbb{1} - \tilde{\Pi}_j)) \right) \quad (34)$$

$$\stackrel{(a)}{=} \min(\pi_i, \pi_j) \left(\text{tr}(\hat{\rho}_i^{\otimes n}(\mathbb{1} - \tilde{\Pi}_i)) + \text{tr}(\hat{\rho}_j^{\otimes n} \tilde{\Pi}_i) \right) \quad (35)$$

where (a) is because $\{\tilde{\Pi}_i, \tilde{\Pi}_j\}$ is a POVM by construction.

Reduction to classical hypothesis testing: We now construct a lower bound on the probability of error for any binary hypothesis test between $\hat{\rho}_i^{\otimes n}$ and $\hat{\rho}_j^{\otimes n}$. Let $\{\Pi_i, \mathbb{1} - \Pi_i\}$ be any POVM for discriminating between $\hat{\rho}_i^{\otimes n}$ and $\hat{\rho}_j^{\otimes n}$. Observe that

$$\text{tr}((\mathbb{1} - \Pi_i) \hat{\rho}_i^{\otimes n}) + \text{tr}(\Pi_i \hat{\rho}_j^{\otimes n}) = 1 - \text{tr}(\Pi_i (\hat{\rho}_j^{\otimes n} - \hat{\rho}_i^{\otimes n})) \quad (36)$$

$$\geq 1 - \max_{\mathbf{0} \leq \Pi \leq \mathbb{1}} \text{tr}(\Pi (\hat{\rho}_j^{\otimes n} - \hat{\rho}_i^{\otimes n})) \quad (37)$$

$$= \text{tr}((\mathbb{1} - \Pi^*) \rho + i^{\otimes n}) + \text{tr}(\Pi^* \hat{\rho}_j^{\otimes n}), \quad (38)$$

where we note that $\max_{\mathbf{0} \leq \Pi \leq \mathbb{1}} \text{tr}(\Pi (\hat{\rho}_j^{\otimes n} - \hat{\rho}_i^{\otimes n})) = \frac{1}{2} \|\hat{\rho}_i^{\otimes n} - \hat{\rho}_j^{\otimes n}\|_1$ and the optimizer is $\Pi^* = \{\hat{\rho}_j^{\otimes n} - \hat{\rho}_i^{\otimes n} > 0\}$, which is the Holevo-Helstrom test, is indeed a Projection-Valued Measure (PVM) [21, Chapter IV.2], [22]. Without loss of generality, we shall develop a lower bound on the probability of error for any PVM $\{\Lambda_i, \mathbb{1} - \Lambda_i\}$, which then also holds for the optimal test Π^* .

The proof follows [20, Theorem 2.2] to construct a binary classical hypothesis testing while taking into consideration the infinite-dimensional density operators. Consider the spectral decomposition of the density operators $\hat{\rho}_i$ and $\hat{\rho}_j$,

$$\hat{\rho}_i = \sum_k \nu_k^i P_k, \quad (39)$$

$$\hat{\rho}_j = \sum_k \nu_k^j Q_k, \quad (40)$$

where $\{P_k\}_{k \in \mathbb{N}}$ and $\{Q_k\}_{k \in \mathbb{N}}$ are sets of finite-dimensional projections corresponding to eigen-subspaces and $\nu_k^i, \nu_k^j \in [0, 1]$ are the respective eigenvalues. The number of projections is finite because trace-class

operators are compact operators. Let Λ_i be defined by choosing a subset of Fock states. Then

$$\alpha \triangleq \text{tr}((\mathbb{1} - \Lambda_i) \hat{\rho}_i) \quad (41)$$

$$= \sum_k \nu_k^i \text{tr}((\mathbb{1} - \Lambda_i) P_k) \quad (42)$$

$$= \sum_k \sum_m \nu_k^i \text{tr}((\mathbb{1} - \Lambda_i) P_k Q_m). \quad (43)$$

Similarly,

$$\beta \triangleq \text{tr}(\Lambda_i \hat{\rho}_j) \quad (44)$$

$$= \sum_m \sum_k \nu_m^j \text{tr}(\Lambda_i P_k Q_m). \quad (45)$$

Combining the obtained identities

$$\alpha + \beta = \sum_k \sum_m (\nu_k^i \text{tr}((\mathbb{1} - \Lambda_i) P_k Q_m) + \nu_m^j \text{tr}(\Lambda_i P_k Q_m)) \quad (46)$$

$$\geq \sum_{k,m} \min(\nu_k^i, \nu_m^j) \text{tr}(P_k Q_m), \quad (47)$$

Since $\{P_k\}_k$ and $\{Q_m\}_m$ are finite-dimensional projections, making $0 \leq \text{tr}(P_k Q_m) < \infty$, then

$$p_{k,m} \triangleq \nu_k^i \text{tr}(P_k Q_m), \quad \forall k, m \in \mathbb{N} \quad (48)$$

$$q_{k,m} \triangleq \nu_m^j \text{tr}(P_k Q_m), \quad \forall k, m \in \mathbb{N} \quad (49)$$

define valid probability distributions on \mathbb{N}^2 . Indeed

$$\sum_{k,m} p_{k,m} = \sum_k \lambda_k^i \sum_m \text{tr}(P_k Q_m) \quad (50)$$

$$= \sum_k \lambda_k^i \text{tr}(P_k) \quad (51)$$

$$= \text{tr}(\hat{\rho}_i) \quad (52)$$

$$= 1 \quad (53)$$

and similarly for $\{q_{k,m}\}_{(k,m) \in \mathbb{N}^2}$. Hence

$$\alpha + \beta \geq \sum_{k,m} \min(p_{k,m}, q_{k,m}) \quad (54)$$

For the hypothesis test between the states $\hat{\rho}_i^{\otimes n}$ and $\hat{\rho}_j^{\otimes n}$ the corresponding classical probability distributions become $p^{\otimes n}$ and $q^{\otimes n}$. By [20, Theorem 2.1], for any sequence of projections $\{\Lambda_{i,n}\}_{n \in \mathbb{N}}$,

$$\limsup_{n \rightarrow \infty} -\frac{1}{n} \log(\text{tr}((\mathbb{1} - \Pi_i) \hat{\rho}_i^{\otimes n}) + \text{tr}(\Pi_j \hat{\rho}_j^{\otimes n})) \leq \lim_{n \rightarrow \infty} -\frac{1}{n} \log \|p^{\otimes n} - q^{\otimes n}\|_1 \quad (55)$$

$$= -\inf_{s \in [0,1]} \log \left(\sum_{k,m} p_{k,m}^s q_{k,m}^{1-s} \right). \quad (56)$$

We note that,

$$\sum_{k,m} p_{k,m}^s q_{k,m}^{1-s} = \sum_{k,m} (\nu_k^i)^s (\nu_m^j)^s \text{tr} (P_k Q_m), \quad (57)$$

$$= \text{tr} \left(\sum_k (\nu_k^i)^s P_k (\nu_m^j)^{1-s} Q_m \right), \quad (58)$$

$$= \text{tr} (\hat{\rho}_i^s \hat{\rho}_j^{1-s}). \quad (59)$$

Since this bound is true for all pairs, (i, j) , we obtain

$$\lim_{n \rightarrow \infty} -\frac{1}{n} \log P_e^n (\{\pi_i \hat{\rho}_i^{\otimes n}\}_{i=1}^m) \leq \min_{(i,j): i \neq j} \max_{s \in [0,1]} -\log \text{tr} (\hat{\rho}_i^s \hat{\rho}_j^{1-s}). \quad (60)$$

4 Joint Communication and Sensing over Entanglement Assisted Bosonic Channels

Our main result for joint communication and sensing is the characterization of the achievable rate/error-exponent region given in the following theorem.

Theorem 4.1. *The set of achievable rate/error-exponent pairs includes the set*

$$\mathcal{C}_{\text{JBCS}} = \bigcup_{\lambda \in [0,1]} \bigcup_{\substack{N_S, N_m \in [0, N]: \\ N_S + N_m \leq N}} \left\{ \begin{array}{l} (R, E) \in \mathbb{R}_+^2 : \\ R \leq \lambda \chi(\{\frac{1}{2\pi}, \hat{\rho}_{BI}^\theta\}) (N) + (1-\lambda) \chi(\{\frac{1}{2\pi}, \hat{\rho}_B^\theta\}) (N_S, N_m) \\ E \leq \lambda E_{\text{nQI}}(N) + (1-\lambda) E_{\text{QI}}^d(N_S, N_m) \end{array} \right\}, \quad (61)$$

where

$$\hat{\rho}_{BI}^\theta = \hat{U}_\theta \otimes \mathbb{1}_I \left(\text{tr}_D \left(\left(\left(\mathcal{L}_{A \rightarrow BD}^{(\eta, N_{\text{th}}/\eta)} \right) \otimes \mathbb{1}_I \right) \hat{\rho}_{SI} \right) \right) \hat{U}_\theta^\dagger \otimes \mathbb{1}, \quad (62)$$

$$\hat{\rho}_B^\theta = \hat{D} \left(\sqrt{N_m} e^{i\theta} \right) \left(\text{tr}_D \left(\left(\left(\mathcal{L}_{A \rightarrow BD}^{(\eta, N_{\text{th}}/\eta)} \right) \otimes \mathbb{1}_I \right) \hat{\rho}_{SI} \right) \right) \hat{D} \left(\sqrt{N_m} e^{i\theta} \right)^\dagger, \quad (63)$$

$$E_{\text{nQI}}(N) = 2 \log \left(\sqrt{(1 + N_{1-\eta})(1 + N_{\text{th}})} - \sqrt{N_{1-\eta} N_{\text{th}}} \right), \quad (64)$$

$$E_{\text{QI}}^d(N_S, N_m) = -\log Q_{0.5}(\hat{\rho}_{RI} \otimes \hat{\rho}_{\text{th}}(N_{\text{th}}) \| \hat{\rho}_{\text{th}}(N_{\text{th}}) \otimes \hat{\rho}_{RI}), \quad (65)$$

$$\hat{\rho}_{RI} = \text{tr}_B \left(\left(\left(\mathcal{L}_{A \rightarrow BD}^{(\eta, N_{\text{th}}/\eta)} \right) \otimes \mathbb{1}_I \right) \hat{\rho}_{SI} \right), \quad (66)$$

and $g(N) = (N+1) \log(N+1) - N \log N$, $N_t \triangleq t N_S + (1-t) \frac{N_{\text{th}}}{\eta}$ for $t \in [0, 1]$, $D = \sqrt{(N + N_\eta + 1)^2 - 4\eta N(N+1)}$.

Proof. The proof is provided in Section 5. ■

Focusing on the region $(1-\eta)$, $N \ll 1$ and $N_{\text{th}} \gg 1$, in which entanglement assistance provides the greatest enhancement, a simplified and more explicit achievable rate/error-exponent region is given in the following theorem.

Theorem 4.2. *In the region $(1 - \eta), N \ll 1$ and $N_{\text{th}} \gg 1$, the set of achievable rate/error-exponent pairs includes the set*

$$\mathcal{C}_{\text{JBCS}} = \bigcup_{\lambda \in [0,1]} \bigcup_{\substack{N_S, N_m \in [0, N]: \\ N_S + N_m \leq N}} \left\{ \begin{array}{l} (R, E) \in \mathbb{R}_+^2 : \\ R \leq \lambda C_{\text{EA}}(N) + (1 - \lambda) R_{\text{ua}}(N_S, N_m) \\ E \leq \lambda E_{\text{nQI}}(N) + (1 - \lambda) E_{\text{QI}}^{\text{d}}(N_S, N_m) \end{array} \right\}, \quad (67)$$

where

$$C_{\text{EA}}(N) = g(N) + g(N_\eta) - g\left(\frac{D + N_\eta - N - 1}{2}\right) - g\left(\frac{D - N_\eta + N - 1}{2}\right), \quad (68)$$

$$R_{\text{ua}}(N_S, N_m) = \eta N_m \log\left(1 + \frac{1}{N_\eta}\right) + \frac{\eta N_m}{N_\eta + 1} - (N_\eta + \eta N_m) \log\left(1 + \frac{\eta N_m}{N_\eta(N_\eta + 1)}\right), \quad (69)$$

$$E_{\text{nQI}}(N) = \left(\frac{(1 - \eta)N}{2N_{\text{th}}}\right)^2, \quad (70)$$

$$E_{\text{QI}}^{\text{d}}(N_S, N_m) = \frac{1 - \eta}{N_{\text{th}}} \left(2N_S + \frac{N_m}{2}\right), \quad (71)$$

and $g(N) = (N + 1) \log(N + 1) - N \log N$, $N_t \triangleq tN_S + (1 - t)\frac{N_{\text{th}}}{\eta}$ for $t \in [0, 1]$, $D = \sqrt{(N + N_\eta + 1)^2 - 4\eta N(N + 1)}$.

Proof. The proof is provided in Section 5. ■

Remark 4.3. *When the entanglement is kept for ranging, the communication channel is equivalent to $\mathcal{L}_{A \rightarrow BD}^{\eta, \eta N_S / (1 - \eta) + N_{\text{th}} / \eta}$. Therefore, N_S acts as additional noise that hurts the performance of unassisted communication.*

We illustrate Theorem 4.1 and 4.2 with a few numerical examples. The numerical result of the rate/error-exponent region corresponding to 4.1 compared against time-sharing is shown in Fig 2. Here, time-sharing refers to the setting $N_S = N$ when entanglement is kept for sensing. Individual trade-off regions for fixed values of λ along the time-sharing curve are shown in Fig. 3. Similarly, the numerical illustration of the rate/error-exponent region corresponding to 4.2 compared to time-sharing is shown in Fig. 4. The comparison between $\chi\left(\left\{\frac{1}{2\pi}, \hat{\rho}_B^\theta\right\}\right)$, $\chi\left(\left\{\frac{1}{\pi N} \exp\left(-\frac{|\alpha|^2}{N}\right), \hat{\rho}_B^\alpha\right\}\right)$ and $R_{\text{ua}}(0, N)$ is shown in Fig. 5. Although we cannot use Gaussian modulated coherent states, corresponding to the ensemble $\left\{\frac{1}{\pi N_m} \exp\left(-\frac{|\alpha|^2}{N_m}\right), \rho_B^\alpha\right\}$, for unassisted communication because of the limitations of Theorem 3.3, Fig. 5 shows that R_{ua} approximates $\chi\left(\left\{\frac{1}{2\pi}, \hat{\rho}_B^\theta\right\}\right)$ and both approximate $\chi\left(\left\{\frac{1}{\pi N} \exp\left(-\frac{|\alpha|^2}{N}\right), \hat{\rho}_B^\alpha\right\}\right)$. The numerical comparison of Quantum Illumination (QI) error-exponents and E_{nQI} against their approximations in Theorem 4.2 is shown in Fig. 6. In here, $E_{\text{QI}}(N_S)$ refers to the mean independent part of the Quantum Chernoff bound between Gaussian states, $-\log \bar{Q}_s$ for \bar{Q}_s defined in [23], and $E_{\text{QI,d}}$ refers to the mean dependent part of the Quantum Chernoff bound. Considering Fig. 5 and 6, the operating regime of the numerical results in Fig. 2 is when the rate approximations still hold but the exponent approximations no longer hold. However, the entanglement assistance still enhances both tasks and which corresponds to a rate/error-exponent region that surpasses time-sharing. When the approximations are valid, trade-off reduces to time-sharing. In the regime where the approximations work entanglement provides significant enhancements in both tasks compared to their unassisted counterparts so that there is no benefit of unassisted communication. Not apparent in the results themselves is a characterization of the ensemble $\chi\left(\left\{\frac{1}{2\pi}, \hat{\rho}_B^\theta\right\}\right)$ in the Fock basis. This characterization plays a crucial role in developing approximations and offering numerical stability in our numerical illustrations.

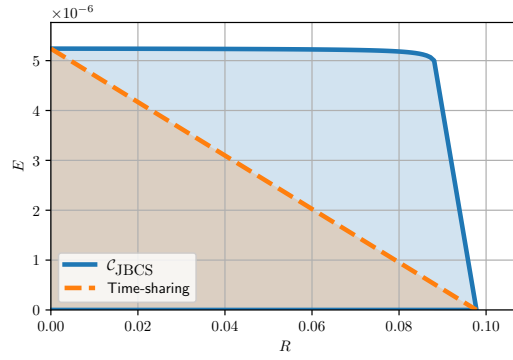


Figure 2: Comparison of the region corresponding to Theorem 4.1 against Time-sharing for $N = 10$, $N_{\text{th}} = 10^4$ and $\eta = 0.99$

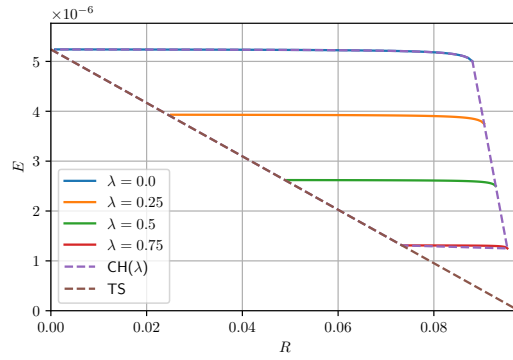


Figure 3: Trade-off regions corresponding to Theorem 4.1 along Time-sharing curve for $N = 10$, $N_{\text{th}} = 10^4$ and $\eta = 0.99$

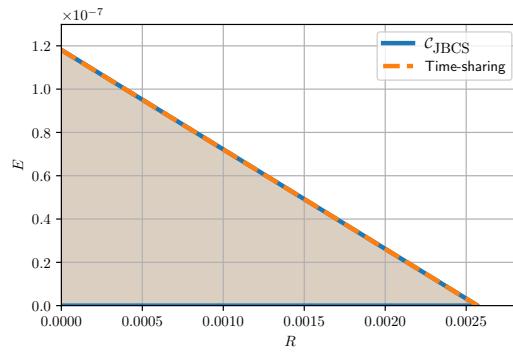


Figure 4: Comparison of the region corresponding to Theorem 4.2 against Time-sharing for $N = 0.1$, $N_{\text{th}} = 10^4$ and $\eta = 0.99$

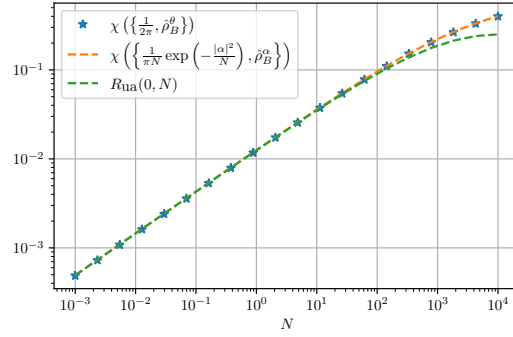


Figure 5: Comparison of $\chi\left(\left\{\frac{1}{2\pi}, \hat{\rho}_B^\theta\right\}\right)$, $\chi\left(\left\{\frac{1}{\pi N} \exp\left(-\frac{|\alpha|^2}{N}\right), \hat{\rho}_B^\alpha\right\}\right)$ and $R_{\text{ua}}(0, N)$ for $N_{\text{th}} = 10^4$ and $\eta = 0.99$

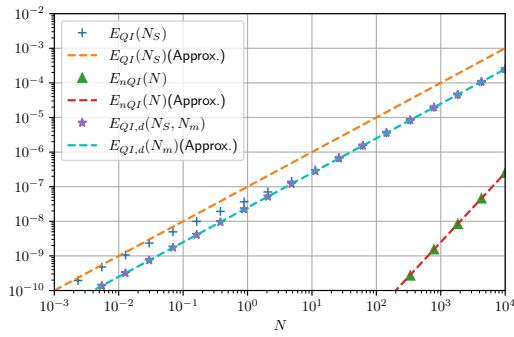


Figure 6: Comparison of $E_{\text{nQI}}(N)$, $E_{\text{QI}}(N_S)$, $E_{\text{QI}}(N_S, N_m)$ and their approximations for $N_{\text{th}} = 10^4$ and $\eta = 0.99$

5 Proofs

We separate the proofs of Theorem 4.1 and 4.2 into three parts; first, we separately show how each scheme performs when entanglement is shared with only transmitter or receiver and then show how to combine those results.

5.1 Unassisted Communication and QI

5.1.1 Unassisted Communication

For unassisted communication encoder is using a displaced phase modulation on the signal part of the TMSV. The displacement is crucial since from Bob's perspective the signal state is a thermal state with mean photon number N_S and a pure phase modulation does not change the state. Formally the displaced phase modulation is defined as

$$\hat{\rho}_{AI}^\theta = D(\alpha_\theta) \otimes \mathbb{1} \hat{\rho}_{SI} D(\alpha_\theta)^\dagger \otimes \mathbb{1}, \quad (72)$$

where $\hat{\rho}_{SI} = |\psi\rangle\langle\psi|_{SI}$, $\alpha_\theta = |\alpha| e^{i\theta}$ for $\theta \in [0, 2\pi)$. Bob's channel output is

$$\hat{\rho}_B^\theta = D(\sqrt{\eta}\alpha_\theta) \hat{\rho}_{\text{ch}}(N_\eta) D(\sqrt{\eta}\alpha_\theta)^\dagger. \quad (73)$$

We first provide a characterization of Bob's received state in the Fock basis.

Lemma 5.1. *Under displaced phase modulation, the mixed state observed by Bob is given as*

$$\begin{aligned} \hat{\rho}_B &= \frac{1}{2\pi} \int_0^{2\pi} \hat{\rho}_B^\theta d\theta \\ &= \sum_{n=0}^{\infty} \exp\left(-\frac{\eta|\alpha|^2}{N_\eta}\right) \frac{N_\eta^n}{(N_\eta+1)^{n+1}} {}_1F_1\left(n+1; 1; \frac{\eta|\alpha|^2}{N_\eta(N_\eta+1)}\right) |n\rangle\langle n|, \end{aligned}$$

where ${}_1F_1(a; b; z) = \sum_{k=0}^{\infty} \frac{a^{(k)} z^k}{b^{(k)} k!}$ is the confluent hypergeometric function.

Proof. For a given θ , coherent state representation of Bob's channel output is

$$\hat{\rho}_B^\theta = \frac{1}{\pi N_\eta} \int \exp\left(-\frac{|\beta - \sqrt{\eta}\alpha_\theta|^2}{N_\eta}\right) |\beta\rangle\langle\beta| d^2\beta. \quad (74)$$

Looking at the Fock basis coefficients

$$\begin{aligned} \langle n | \hat{\rho}_B^\theta | m \rangle &= \frac{1}{\pi N_\eta} \int \exp \left(-\frac{|\beta|^2 + \eta |\alpha|^2 - 2\sqrt{\eta} |\alpha| (\beta_R \cos(\theta) + \beta_I \sin(\theta))}{N_\eta} \right) \langle n | \beta \rangle \langle \beta | m \rangle d^2 \beta \\ &= \frac{1}{\pi N_\eta} \int \exp \left(-\frac{|\beta|^2 + \eta |\alpha|^2 - 2\sqrt{\eta} |\alpha| (\beta_R \cos(\theta) + \beta_I \sin(\theta))}{N_\eta} \right) \frac{\beta^n (\beta^*)^m}{\sqrt{n! m!}} \exp(-|\beta|^2) d^2 \beta \end{aligned} \quad (75)$$

$$\stackrel{(a)}{=} \frac{\exp \left(-\frac{\eta |\alpha|^2}{N_\eta} \right)}{\pi N_\eta \sqrt{n! m!}} \int_0^\infty \int_0^{2\pi} \exp \left(-\frac{N_\eta + 1}{N_\eta} r^2 + \frac{2\sqrt{\eta} |\alpha| r}{N_\eta} \cos(\phi - \theta) \right) r^{n+m+1} e^{i(n-m)\phi} d\phi dr \quad (77)$$

$$= \frac{2 \exp \left(-\frac{\eta |\alpha|^2}{N_\eta} \right)}{N_\eta \sqrt{n! m!}} \quad (78)$$

$$\times \int_0^\infty \exp \left(-\frac{N_\eta + 1}{N_\eta} r^2 \right) r^{n+m+1} \left(\frac{1}{2\pi} \int_0^{2\pi} \exp \left(\frac{2\sqrt{\eta} |\alpha| r}{N_\eta} \cos(\phi - \theta) + i(n-m)\phi \right) d\phi \right) dr, \quad (79)$$

where (a) is the change to polar coordinates. Looking at the inner integral

$$\frac{1}{2\pi} \int_0^{2\pi} \exp \left(\frac{2\sqrt{\eta} |\alpha| r}{N_\eta} \cos(\phi - \theta) + i(n-m)\phi \right) d\phi \quad (80)$$

$$\stackrel{\gamma = \phi - \theta}{=} \frac{1}{2\pi} \int_{-\theta}^{2\pi - \theta} \exp \left(\frac{2\sqrt{\eta} |\alpha| r}{N_\eta} \cos(\gamma) + i(n-m)\gamma \right) d\phi e^{i(n-m)\theta} \quad (81)$$

$$= I_{n-m} \left(\frac{2\sqrt{\eta} |\alpha| r}{N_\eta} \right) e^{i(n-m)\theta}. \quad (82)$$

Then, the Fock basis coefficients of $\hat{\rho}_B^\theta$ become

$$\langle n | \hat{\rho}_B^\theta | m \rangle = \frac{2 \exp \left(-\frac{\eta |\alpha|^2}{N_\eta} + i(n-m)\theta \right)}{N_\eta \sqrt{n! m!}} \int_0^\infty \exp \left(-\frac{N_\eta + 1}{N_\eta} r^2 \right) r^{n+m+1} I_{n-m} \left(\frac{2\sqrt{\eta} |\alpha| r}{N_\eta} \right) dr. \quad (83)$$

When taking the mixture with respect to θ , the only term that depends on θ is $e^{i(n-m)\theta}$, hence

$$\langle n | \hat{\rho}_B | m \rangle = \frac{1}{2\pi} \int_0^{2\pi} \langle n | \hat{\rho}_B^\theta | m \rangle d\theta \quad (84)$$

$$= \delta_{n-m} \frac{2 \exp \left(-\frac{\eta |\alpha|^2}{N_\eta} \right)}{N_\eta n!} \int_0^\infty \exp \left(-\frac{N_\eta + 1}{N_\eta} r^2 \right) r^{2n+1} I_0 \left(\frac{2\sqrt{\eta} |\alpha| r}{N_\eta} \right) dr, \quad (85)$$

where we have used the series expansion $I_0(z) = \sum_{k=0}^{\infty} \frac{1}{(k!)^2} \left(\frac{z}{2}\right)^{2k}$. Hence,

$$\langle n|\hat{\rho}_B|n\rangle = \langle n|\hat{\rho}_B^\theta|n\rangle \quad (86)$$

$$= \frac{\exp\left(-\frac{\eta|\alpha|^2}{N_\eta}\right)}{N_\eta n!} \sum_{k=0}^{\infty} \frac{1}{(k!)^2} \left(\frac{\sqrt{\eta}|\alpha|}{N_\eta}\right)^{2k} \int_0^\infty r^{2(n+k)} \exp\left(-\frac{N_\eta+1}{N_\eta}r^2\right) 2r dr \quad (87)$$

$$= \frac{\exp\left(-\frac{\eta|\alpha|^2}{N_\eta}\right)}{N_\eta n!} \sum_{k=0}^{\infty} \frac{1}{(k!)^2} \left(\frac{\sqrt{\eta}|\alpha|}{N_\eta}\right)^{2k} \left(\frac{N_\eta}{N_\eta+1}\right)^{n+k+1} \int_0^\infty u^{n+k} \exp(-u) du \quad (88)$$

$$= \exp\left(-\frac{\eta|\alpha|^2}{N_\eta}\right) \frac{N_\eta^n}{(N_\eta+1)^{n+1}} \sum_{k=0}^{\infty} \binom{n+k}{k} \frac{1}{k!} \left(\frac{\eta|\alpha|^2}{N_\eta(N_\eta+1)}\right)^k \quad (89)$$

$$= \exp\left(-\frac{\eta|\alpha|^2}{N_\eta}\right) \frac{N_\eta^n}{(N_\eta+1)^{n+1}} \sum_{k=0}^{\infty} \frac{(n+1)_{(k)}}{(1)_{(k)}k!} \left(\frac{\eta|\alpha|^2}{N_\eta(N_\eta+1)}\right)^k \quad (90)$$

$$= \exp\left(-\frac{\eta|\alpha|^2}{N_\eta}\right) \frac{N_\eta^n}{(N_\eta+1)^{n+1}} {}_1F_1\left(n+1; 1; \frac{\eta|\alpha|^2}{N_\eta(N_\eta+1)}\right) \quad (91)$$

■

We use Lemma 5.1 to lower bound the associated Holevo information. In order to calculate the Holevo information, we need the following lemma.

Lemma 5.2.

$$\frac{{}_1F_1(\alpha+1, \beta, z)}{{}_1F_1(\alpha, \beta, z)} \leq 1 + \frac{z}{\beta} \quad (92)$$

for $\alpha, \beta \in \mathbb{N}_*$ and $z \in \mathbb{R}_+$.

Proof. From the first recurrence relation in [24] we have

$$\beta {}_1F_1(\alpha+1; \beta; z) - \beta {}_1F_1(\alpha; \beta; z) = z {}_1F_1(\alpha; \beta+1; z) \quad (93)$$

$$\leq z {}_1F_1(\alpha; \beta; z). \quad (94)$$

The inequality is due to monotonicity of the confluent hypergeometric function in the second argument when $\alpha \geq 1$ and $z > 0$. After rearranging terms, the inequality becomes

$$\beta {}_1F_1(\alpha+1; \beta; z) \leq (\beta+z) {}_1F_1(\alpha; \beta; z). \quad (95)$$

■

Using the above result, we obtain the following bound for the Holevo information.

Lemma 5.3. *Under displaced phase modulation, the Holevo information is lower bounded by*

$$S(\hat{\rho}_B) - \frac{1}{2\pi} \int_0^{2\pi} S(\hat{\rho}_B^\theta) d\theta \geq \frac{\eta N_m}{N_\eta+1} + \eta N_m \log\left(1 + \frac{1}{N_\eta}\right) - (N_\eta + \eta N_m) \log\left(1 + \frac{\eta N_m}{N_\eta(N_\eta+1)}\right), \quad (96)$$

$\forall N_S, N_m, N_{th} \in \mathbb{R}_+$ and $\eta \in [0, 1]$.

Proof. $\hat{\rho}_B^\theta$ is a displaced thermal state with mean photon number N_η , $\forall \theta \in [0, 2\pi)$, hence $S(\hat{\rho}_B^\theta) = g(N_\eta)$. For the first term, we have

$$\begin{aligned} S(\hat{\rho}_B) &= -\exp\left(-\frac{\eta|\alpha|^2}{N_\eta}\right) \sum_{n=0}^{\infty} \frac{N_\eta^n}{(N_\eta+1)^{n+1}} {}_1F_1\left(n+1; 1; \frac{\eta|\alpha|^2}{N_\eta(N_\eta+1)}\right) \\ &\quad \times \left(-\frac{\eta|\alpha|^2}{N_\eta} - n \log\left(\frac{N_\eta+1}{N_\eta}\right) - \log(N_\eta+1) - \log {}_1F_1\left(n+1; 1; \frac{\eta|\alpha|^2}{N_\eta(N_\eta+1)}\right)\right) \end{aligned} \quad (97)$$

$$\begin{aligned} &= \frac{\eta|\alpha|^2}{N_\eta} + g(N_\eta) + \eta|\alpha|^2 \log\left(1 + \frac{1}{N_\eta}\right) \\ &\quad - \exp\left(-\frac{\eta|\alpha|^2}{N_\eta}\right) \sum_{n=0}^{\infty} \frac{N_\eta^n}{(N_\eta+1)^{n+1}} {}_1F_1\left(n+1; 1; \frac{\eta|\alpha|^2}{N_\eta(N_\eta+1)}\right) \\ &\quad \times \log {}_1F_1\left(n+1; 1; \frac{\eta|\alpha|^2}{N_\eta(N_\eta+1)}\right). \end{aligned} \quad (98)$$

From Lemma 5.2, we obtain

$$\frac{{}_1F_1(n+1; 1; z)}{{}_1F_1(1; 1; z)} = \prod_{i=1}^n \frac{{}_1F_1(i+1; 1; z)}{{}_1F_1(i; 1; z)} \quad (99)$$

$$\leq \prod_{i=1}^n (1+z) \quad (100)$$

$$= (1+z)^n. \quad (101)$$

Using this relation, the last part of (98) becomes

$$\begin{aligned} &-\exp\left(-\frac{\eta|\alpha|^2}{N_\eta}\right) \sum_{n=0}^{\infty} \frac{N_\eta^n}{(N_\eta+1)^{n+1}} {}_1F_1\left(n+1; 1; \frac{\eta|\alpha|^2}{N_\eta(N_\eta+1)}\right) \\ &\quad \times \log {}_1F_1\left(n+1; 1; \frac{\eta|\alpha|^2}{N_\eta(N_\eta+1)}\right) \end{aligned} \quad (102)$$

$$\begin{aligned} &\stackrel{(a)}{\geq} -\exp\left(-\frac{\eta|\alpha|^2}{N_\eta}\right) \sum_{n=0}^{\infty} \frac{N_\eta^n}{(N_\eta+1)^{n+1}} {}_1F_1\left(n+1; 1; \frac{\eta|\alpha|^2}{N_\eta(N_\eta+1)}\right) \\ &\quad \times \left(n \log\left(1 + \frac{\eta|\alpha|^2}{N_\eta(N_\eta+1)}\right) + \frac{\eta|\alpha|^2}{N_\eta(N_\eta+1)}\right) \end{aligned} \quad (103)$$

$$= -(N_\eta + \eta|\alpha|^2) \log\left(1 + \frac{\eta|\alpha|^2}{N_\eta(N_\eta+1)}\right) - \frac{\eta|\alpha|^2}{N_\eta(N_\eta+1)} \quad (104)$$

By lower bounding (98) by (104), subtracting $g(N_\eta)$ and substituting $|\alpha|^2 = N_m$ we obtain the desired result. \blacksquare

Note that Lemma 5.3 is a bound that holds without making approximations or assuming low signal to high noise regime.

5.1.2 Quantum Illumination

For the detection, each mode except the true hypothesis is a thermal state with mean photon number N_{th} and the true hypothesis is a Gaussian state $\hat{\rho}_{RI}^\theta$ with mean vector (r_{RI}^θ) and covariance matrix (V_{RI}^θ)

$$r_{RI}^\theta = -2\sqrt{(1-\eta)N_m} \begin{bmatrix} \cos(\theta) \\ \sin(\theta) \\ 0 \\ 0 \end{bmatrix} \quad (105)$$

$$V_{RI}^\theta = \begin{bmatrix} EI & CR_\theta \\ CR_\theta & SI \end{bmatrix} \quad (106)$$

where $\mathbf{R}_\theta = \begin{bmatrix} \cos \theta & \sin \theta \\ \sin \theta & -\cos \theta \end{bmatrix}$, $E = 2N_{1-\eta} + 1$, $C = 2(1-\eta)\sqrt{N_S(N_S+1)}$ and $S = 2N_S + 1$.

Since we do not know which mode is displaced, we cannot get rid of the displacement. However, we can get rid of its phase by applying the unitaries $\left\{ \exp(-i\theta \hat{N}_k) \right\}_{k \in [1, m]}$ to each received mode and it will cancel the phase of the displacement of the true hypothesis and the remaining modes will be unaffected since they are diagonal in Fock basis. Then the detection problem reduces to hypothesis testing between n copies of the states

$$\left\{ \hat{\rho}_{\text{th}}(N_{\text{th}})^{\otimes(h-1)} \otimes \hat{\rho}_{RI} \otimes \hat{\rho}_{\text{th}}^{\otimes(m-h)}(N_{\text{th}}) \right\}_{h=1}^m. \quad (107)$$

By applying Theorem 3.1, the error exponent is given as

$$E_{Q_I}^d(N_S, N_m) = - \min_{s \in [0,1]} \log Q_s(\hat{\rho}_{\text{th}}(N_{\text{th}}) \otimes \hat{\rho}_{RI} \| \hat{\rho}_{RI} \otimes \hat{\rho}_{\text{th}}(N_{\text{th}})). \quad (108)$$

Following the approach of [23] the Chernoff bound between two n -mode Gaussian states with covariance matrices $V_1 = S_1 \left(\bigoplus_{i=1}^n \nu_i^1 \mathbf{I}_2 \right) S_1^T$ and $V_2 = S_2 \left(\bigoplus_{i=1}^n \nu_i^2 \mathbf{I}_2 \right) S_2^T$ is given as

$$Q_s = \bar{Q}_s \exp \left(-\frac{1}{2} d^T (V_1(s) + V_2(1-s))^{-1} d \right) \quad (109)$$

where

$$V_i(s) = S_i \left(\bigoplus_{i=1}^n \Lambda_s(\nu_i^i) \mathbf{I}_2 \right) S_i^T \quad (110)$$

$$\Lambda_s(x) = \frac{(x+1)^s + (x-1)^s}{(x+1)^s - (x-1)^s} \quad (111)$$

The exponent corresponding to the first term, \bar{Q}_s in (109), is calculated in [12] as

$$- \min_{s \in [0,1]} \log \bar{Q}_s = - \log \bar{Q}_{\frac{1}{2}} \quad (112)$$

$$\approx \frac{2(1-\eta)N_S}{N_{\text{th}}}, \quad (113)$$

for $N_S, (1-\eta) \ll 1$ and $N_{\text{th}} \gg 1$. For the second term where in (109) d is the difference between the mean vectors, we have in our case

$$d = -2\sqrt{(1-\eta)N_m} [1 \ 0 \ -1 \ 0 \ 0 \ 0]^T. \quad (114)$$

We have numerically confirmed that $s = 0.5$ seems optimal for the displacement term in the Quantum Chernoff bound (109). Assuming both N_S and N_m are $\mathcal{O}(N)$, we obtain the first order term in $1 - \eta$ and N_S, N_m as

$$\frac{1}{2}d^T (V_1(0.5) + V_2(0.5))^{-1} d \approx \frac{2(1 - \eta)N_m}{1 + 2N_{\text{th}} + 2\sqrt{N_{\text{th}}(N_{\text{th}} + 1)}}. \quad (\text{II5})$$

As in [12] by assuming $N_{\text{th}} \gg 1$ we obtain

$$\frac{1}{2}d^T (V_1(0.5) + V_2(0.5))^{-1} d \approx \frac{(1 - \eta)N_m}{2N_{\text{th}}}. \quad (\text{II6})$$

Hence, the error exponent becomes

$$E_{QI}^d(N_S, N_m) = \frac{1 - \eta}{N_{\text{th}}} \left(2N_S + \frac{N_m}{2} \right). \quad (\text{II7})$$

5.2 Entanglement Assisted Communication and Unassisted Sensing

5.2.1 Entanglement Assisted Communication

[25, 26] has shown that uniform phase modulation over TMSV, $\hat{U}_\theta |\psi\rangle \langle \phi|_{SI} \hat{U}_\theta^\dagger$ with $\hat{U}_\theta = \exp(i\theta N)$ for $\theta \in [0, 2\pi)$, achieves C_{EA} when $N \ll 1 \ll N_{\text{th}}$ asymptotically.

5.2.2 Unassisted Sensing

Since we are using phase modulation for entanglement assisted communication, the hypothesis testing amounts to distinguishing between n copies of the states

$$\left\{ \hat{\rho}_{\text{th}}(N_{\text{th}})^{\otimes(h-1)} \otimes \hat{\rho}_{\text{th}}(N_{1-\eta}) \otimes \hat{\rho}_{\text{th}}^{\otimes(m-h)} \right\}_{h=1}^m \quad (\text{II8})$$

Let $\hat{\rho}_i \triangleq \hat{\rho}_{\text{th}}(N_{\text{th}})^{\otimes(i-1)} \otimes \hat{\rho}_{\text{th}}(N_{1-\eta}) \otimes \hat{\rho}_{\text{th}}^{\otimes(m-i)}$ for $i \in \llbracket 1, m \rrbracket$. By Theorem 3.1 the unassisted error exponent, E_{nQI} , is given as

$$E_{nQI} = \min_{(i,j):i \neq j} \max_{s \in [0,1]} -\log Q_s(\hat{\rho}_i \| \hat{\rho}_j) \quad (\text{II9})$$

Focusing on the Q_s term, assuming $i < j$ without loss of generality,

$$Q_s(\hat{\rho}_i \| \hat{\rho}_j) = \text{tr}(\hat{\rho}_i^s \hat{\rho}_j^{1-s}) \quad (\text{I20})$$

$$= \left(\prod_{k=1}^{i-1} \text{tr}(\hat{\rho}_{\text{th}}(N_{\text{th}})) \right) \text{tr}(\hat{\rho}_{\text{th}}(N_{1-\eta})^s \hat{\rho}_{\text{th}}(N_{\text{th}})^{1-s}) \left(\prod_{\ell=i+1}^{j-1} \text{tr}(\hat{\rho}_{\text{th}}(N_{\text{th}})) \right) \quad (\text{I21})$$

$$\times \text{tr}(\hat{\rho}_{\text{th}}(N_{\text{th}})^s \hat{\rho}_{\text{th}}(N_{1-\eta})^{1-s}) \left(\prod_{p=j+1}^m \text{tr}(\hat{\rho}_{\text{th}}(N_{\text{th}})) \right) \quad (\text{I22})$$

$$= \text{tr}(\hat{\rho}_{\text{th}}(N_{1-\eta})^s \hat{\rho}_{\text{th}}(N_{\text{th}})^{1-s}) \text{tr}(\hat{\rho}_{\text{th}}(N_{\text{th}})^s \hat{\rho}_{\text{th}}(N_{1-\eta})^{1-s}) \quad (\text{I23})$$

$$= Q_s(\hat{\rho}_{\text{th}}(N_{1-\eta}) \| \hat{\rho}_{\text{th}}(N_{\text{th}})) Q_s(\hat{\rho}_{\text{th}}(N_{\text{th}}) \| \hat{\rho}_{\text{th}}(N_{1-\eta})) \quad (\text{I24})$$

$$= Q_s(\hat{\rho}_{\text{th}}(N_{1-\eta}) \| \hat{\rho}_{\text{th}}(N_{\text{th}})) Q_{1-s}(\hat{\rho}_{\text{th}}(N_{1-\eta}) \| \hat{\rho}_{\text{th}}(N_{\text{th}})) \quad (\text{I25})$$

Observe that (125) does not depend on (i, j) for $i \neq j$. Now focusing on the first term in (125), let $r_1 \triangleq \frac{N_{1-\eta}}{N_{1-\eta}+1}$ and $r_2 \triangleq \frac{N_{\text{th}}}{N_{\text{th}}+1}$, then

$$Q_s(\hat{\rho}_{\text{th}}(N_{1-\eta})\|\hat{\rho}_{\text{th}}(N_{\text{th}})) = (1-r_1)^s(1-r_2)^{1-s} \sum_{n=0}^{\infty} (r_1^s r_2^{1-s})^n \quad (126)$$

$$= \frac{(1-r_1)^s(1-r_2)^{1-s}}{1-r_1^s r_2^{1-s}}. \quad (127)$$

Substituting this into (125),

$$Q_s(\hat{\rho}_i\|\hat{\rho}_j) = \frac{(1-r_1)(1-r_2)}{1+r_1 r_2 - r_1^s r_2^{1-s} - r_1^{1-s} r_2^s} \quad (128)$$

By Theorem 3.1 we need to minimize this quantity, for the optimal $s = s^*$ that minimizes the Chernoff bound

$$\operatorname{argmin}_{s \in [0,1]} \frac{(1-r_1)(1-r_2)}{1+r_1 r_2 - r_1^s r_2^{1-s} - r_1^{1-s} r_2^s} = \operatorname{argmin}_{s \in [0,1]} r_1^s r_2^{1-s} + r_1^{1-s} r_2^s \quad (129)$$

Let $f(s) \triangleq r_1^s r_2^{1-s} + r_1^{1-s} r_2^s$, then

$$f'(s^*) = r_1^{s^*} r_2^{1-s^*} (\log r_1 - \log r_2) + r_1^{1-s^*} r_2^{s^*} (\log r_2 - \log r_1) \quad (130)$$

$$= (r_1^{s^*} r_2^{1-s^*} - r_1^{1-s^*} r_2^{s^*}) (\log r_1 - \log r_2) \quad (131)$$

$$= 0 \quad (132)$$

Since $r_1 \neq r_2$, we must have $r_1^{s^*} r_2^{1-s^*} = r_1^{1-s^*} r_2^{s^*}$. This simplifies to $(r_1 r_2)^{2s^*-1} = 1$ and the solution is $s^* = \frac{1}{2}$. Then the unassisted error exponent is

$$E_{n\text{QI}}(N) = 2 \log \left(1 - \sqrt{\frac{N_{1-\eta} N_{\text{th}}}{(N_{1-\eta}+1)(N_{\text{th}}+1)}} \right) + \log(1+N_{1-\eta}) + \log(1+N_{\text{th}}) \quad (133)$$

$$= 2 \log \left(\sqrt{(1+N_{1-\eta})(1+N_{\text{th}})} - \sqrt{N_{1-\eta} N_{\text{th}}} \right). \quad (134)$$

In the regime $N \ll 1 \ll N_{\text{th}}$ we obtain the approximation

$$E_{n\text{QI}}(N) \approx \left(\frac{(1-\eta)N}{2N_{\text{th}}} \right)^2. \quad (135)$$

5.3 Joint communication and Sensing Region

For a fixed fraction λ of the blocklength n , the idler is shared with the receiver to enhance communication and for the remaining fraction $1 - \lambda$ the idler is kept for enhancing sensing operation. In each case, the detection problem reduces to hypothesis testing with product states since we can eliminate the phase. We can consider the sharing of entanglement as a modulation scheme with fixed type and applying Theorem 3.3 the total exponent becomes

$$E = \min_{(i,j):i \neq j} \max_{s \in [0,1]} (-\lambda \log Q_s(\hat{\rho}_{\text{th}}(N_{1-\eta}) \otimes \hat{\rho}_{\text{th}}(N_{\text{th}})\|\hat{\rho}_{\text{th}}(N_{\text{th}}) \otimes \hat{\rho}_{\text{th}}(N_{1-\eta})) - (1-\lambda) \log Q_s(\hat{\rho}_{RI} \otimes \hat{\rho}_{\text{th}}(N_{\text{th}})\|\hat{\rho}_{\text{th}}(N_{\text{th}}) \otimes \hat{\rho}_{RI})) \quad (136)$$

$$\stackrel{(a)}{=} \lambda E_{n\text{QI}}(N) + (1-\lambda) E_{\text{QI}}^d(N_S, N_m), \quad (137)$$

where (a) is because $s = 0.5$ is optimal for both Chernoff bounds.

Since we are time-sharing between two schemes, the communication rate is the convex combination of the rates in individual schemes,

$$R = \lambda C_{\text{EA}}(N) + (1 - \lambda)(1 - \lambda)R_{ua}(N_S, N_m). \quad (138)$$

Taking the union over $\lambda \in [0, 1]$ and $N_S + N_m \leq N$ completes the proof.

References

- [1] J. Yin, Y. Cao, Y.-H. Li, S.-K. Liao, L. Zhang, J.-G. Ren, W.-Q. Cai, W.-Y. Liu, B. Li, H. Dai, G.-B. Li, Q.-M. Lu, Y.-H. Gong, Y. Xu, S.-L. Li, F.-Z. Li, Y.-Y. Yin, Z.-Q. Jiang, M. Li, J.-J. Jia, G. Ren, D. He, Y.-L. Zhou, X.-X. Zhang, N. Wang, X. Chang, Z.-C. Zhu, N.-L. Liu, Y.-A. Chen, C.-Y. Lu, R. Shu, C.-Z. Peng, J.-Y. Wang, and J.-W. Pan, “Satellite-based entanglement distribution over 1200 kilometers,” *Science*, vol. 356, no. 6343, pp. 1140–1144, Jun. 2017.
- [2] M. Pant, H. Krovi, D. Towsley, L. Tassioulas, L. Jiang, P. Basu, D. Englund, and S. Guha, “Routing entanglement in the quantum internet,” *npj Quantum Information*, vol. 5, no. 1, p. 25, 2019.
- [3] H. He, L. Jiang, Y. Pan, A. Yi, X. Zou, W. Pan, A. E. Willner, X. Fan, Z. He, and L. Yan, “Integrated sensing and communication in an optical fibre,” *Light: Science & Applications*, vol. 12, no. 1, p. 25, Jan 2023.
- [4] M. M. Wilde, M. Tomamichel, S. Lloyd, and M. Berta, “Gaussian hypothesis testing and quantum illumination,” *Phys. Rev. Lett.*, vol. 119, p. 120501, Sep 2017.
- [5] C. Bennett, P. Shor, J. Smolin, and A. Thapliyal, “Entanglement-assisted capacity of a quantum channel and the reverse shannon theorem,” *IEEE Transactions on Information Theory*, vol. 48, no. 10, pp. 2637–2655, Oct 2002.
- [6] S.-Y. Wang, T. Erdođan, U. Pereg, and M. R. Bloch, “Joint quantum communication and sensing,” in *Proc. of IEEE Information Theory Workshop*, Aug. 2022, pp. 506–511.
- [7] P. Munar-Vallespir and J. Nötzel, “Joint communication and sensing over the lossy bosonic quantum channel,” in *Proc. of IEEE 10th World Forum on Internet of Things*, Nov 2024, pp. 1–6.
- [8] M. Ahmadipour, M. Kobayashi, M. Wigger, and G. Caire, “An information-theoretic approach to joint sensing and communication,” *IEEE Transactions on Information Theory*, vol. 70, no. 2, pp. 1124–1146, 2024.
- [9] H. Joudeh and F. M. J. Willems, “Joint communication and binary state detection,” *IEEE Journal on Selected Areas in Information Theory*, vol. 3, no. 1, pp. 113–124, 2022.
- [10] M.-C. Chang, T. Erdođan, S.-Y. Wang, and M. R. Bloch, “Rate and detection error-exponent tradeoffs of joint communication and sensing,” in *2022 2nd IEEE International Symposium on Joint Communications & Sensing (JC&S)*, 2022, pp. 1–6.
- [11] M.-C. Chang, S.-Y. Wang, T. Erdođan, and M. R. Bloch, “Rate and detection-error exponent trade-off for joint communication and sensing of fixed channel states,” *IEEE Journal on Selected Areas in Information Theory*, vol. 4, pp. 245–259, 2023.
- [12] Q. Zhuang, “Quantum ranging with gaussian entanglement,” *Phys. Rev. Lett.*, vol. 126, p. 240501, Jun 2021.

- [13] C. Weedbrook, S. Pirandola, R. García-Patrón, N. J. Cerf, T. C. Ralph, J. H. Shapiro, and S. Lloyd, “Gaussian quantum information,” *Rev. Mod. Phys.*, vol. 84, pp. 621–669, May 2012.
- [14] K. Li, “Discriminating quantum states: The multiple chernoff distance,” *The Annals of Statistics*, vol. 44, no. 4, Aug 2016.
- [15] P. Munar-Vallespir and J. Nötzel, “Joint communication and sensing over the lossy bosonic quantum channel,” in *2024 IEEE 10th World Forum on Internet of Things (WF-IoT)*, Nov 2024, pp. 1–6.
- [16] K. M. R. Audenaert, J. Calsamiglia, R. Muñoz Tápia, E. Bagan, L. Masanes, A. Acín, and F. Verstraete, “Discriminating states: The quantum chernoff bound,” *Phys. Rev. Lett.*, vol. 98, p. 160501, Apr 2007.
- [17] S. Nitinawarat, G. K. Atia, and V. V. Veeravalli, “Controlled sensing for multihypothesis testing,” *IEEE Transactions on Automatic Control*, vol. 58, no. 10, pp. 2451–2464, May 2013.
- [18] F. Hiai, “Quantum f-divergences in von Neumann algebras. I. Standard f-divergences,” *Journal of Mathematical Physics*, vol. 59, no. 10, p. 102202, Sep 2018.
- [19] R. T. Rockafellar, *Convex Analysis*. Princeton: Princeton University Press, 1970.
- [20] M. Nussbaum and A. Szkoła, “Asymptotically Optimal Discrimination between Pure Quantum States,” in *Theory of Quantum Computation, Communication, and Cryptography*. Springer, Berlin, Heidelberg, Apr 2011, pp. 1–8.
- [21] C. W. Helstrom, *Quantum detection and estimation theory*, 1st ed. New York, NY, USA: Academic Press, 1976.
- [22] A. S. Holevo, “Investigations in the General Theory of Statistical Decisions,” *Proceedings of the Steklov Institute of Mathematics*, vol. 124, no. 3, 1978.
- [23] S. Pirandola and S. Lloyd, “Computable bounds for the discrimination of gaussian states,” *Phys. Rev. A*, vol. 78, p. 012331, Jul 2008.
- [24] “NIST Digital Library of Mathematical Functions,” <https://dlmf.nist.gov/>, Release 1.2.2 of 2024-09-15, f. W. J. Olver, A. B. Olde Daalhuis, D. W. Lozier, B. I. Schneider, R. F. Boisvert, C. W. Clark, B. R. Miller, B. V. Saunders, H. S. Cohl, and M. A. McClain, eds.
- [25] H. Shi, Z. Zhang, and Q. Zhuang, “Practical route to entanglement-assisted communication over noisy bosonic channels,” *Phys. Rev. Appl.*, vol. 13, p. 034029, Mar 2020.
- [26] S.-J. Su, S.-Y. Wang, M. R. Bloch, and Z. Zhang, “Achievable entanglement-assisted communication rate using phase-modulated two-mode squeezed vacuum,” *arXiv preprint*, Oct 2024.